

## Redox Study of Polyaniline Derivatives For Potential Uses In Photovoltaic Devices

P.P. Zamora<sup>1</sup>, F.R. Díaz<sup>1</sup>, M.A. del Valle<sup>2</sup>, G. Louarn<sup>3</sup>, L. Cattin<sup>3</sup>  
and J.C. Bernède<sup>4</sup>

<sup>1</sup>Laboratorio de Polímeros, Facultad de Química, Pontificia Universidad Católica de Chile, Vicuña Mackenna 4860, Santiago, Chile. Fax: (+56)2-68644804 E-mail: [ppzamora@uc.cl](mailto:ppzamora@uc.cl)

<sup>2</sup>Pontificia Universidad Católica de Chile, Facultad de Química, Departamento de Química Inorgánica, Laboratorio de Electroquímica de Polímeros, Av. Vicuña Mackenna 4860, Santiago de Chile

<sup>3</sup>Université de Nantes, LUNAM Université, Institut des Matériaux de Nantes, CNRS, 2 rue de la Houssinière, BP 32229, 44322 Nantes cedex 3, France

<sup>4</sup>Université de Nantes, LUNAM Université, MOLTECH-Anjou, CNRS, UMR 6200, 2 rue de la Houssinière, BP 92208, Nantes, F-44000 France

### ABSTRACT

Polyaniline (PANI) derivatives were synthesized using chemical methods by varying the oxidant concentration to favor the quinoids units formation. FT-IR, UV-Vis, and cyclic voltammetry characterization conclusively demonstrated that polymer oxidation becomes more difficult as the size of the substituent increases. At the same time, larger substituent size tends to shift the onset oxidation potential ( $E_{ox}^{on}$ ) toward positive.

Polyaniline derivate polymers were used in photovoltaic devices as electronic donors to study the optimum redox state so as to understand how the presence of quinoid units affects the photovoltaic yield. In previous work we have shown that thiophene or furane aniline based polymers can increase photovoltaic yield of anilines. Quinoid units play an essential role in the behavior of this parameter.

**Keywords:** Onset Oxidation Potential, Polyaniline, Photovoltaic Yield

### INTRODUCTION

Semiconducting polymers have aroused great interest amidst chemists and physicists because these materials have many advantages over traditional metallic conductors [1]. Many types of semiconductive polymers have been synthesized and studied because of their potential applications in rechargeable batteries [2], electrochromic devices [3-5], dye-sensitized solar cells (DSSCs), organic solar cells and organic light emitting diodes [6], among others. These materials are mainly conjugated molecules, where the polymer backbone can turn into an electrically conductive electronic structure. The conductivity in some cases may be similar to that of metals and can be increased or decreased by the

addition of species capable of physically modifying the electrical properties of the chain. The aforementioned process is known as *doping* [3].

The charge generated by the doping process or photoexcitation process must be transported along the polymer network and, therefore, it should have a certain mobility which depends on the resistance of the polymeric chain [7]. The mobility rate-determination step is the process that presents the highest resistance. Charge carrier hopping between chains is directly related to the degree in which these have overlapped, which, in turn, depends on how they are packaged, i.e., inter-chain hopping must be normal to them [8]. In order to achieve efficient charge transport, both for intra- and inter-chain, polyaniline and its derivatives must be in a redox state with quinoid units [9]. These units can be characterized by UV-Vis and FT-IR spectroscopy. The optimum benzenoid/quinoid ratio is 1.46 for UV-Vis spectroscopy and 1:1 in FT-IR spectroscopy [9]. If the oxidant/monomer ratio is not optimum the resulting polymer may be under- or over-oxidized. It is well known that PANI is not efficient as an electron donor in photovoltaic devices because it has a large band gap; nonetheless, the quinoid units trigger the formation of carriers which produce a modest photovoltaic effect. In our previous work, we have shown that the quinoid moieties increases the photovoltaic yield and we have shown that the incorporation of thiophene or furane moieties between aniline rings, trigger a decrease the band gap [10].

In the present work we have synthesized different PANI derivatives Figure 1 and used them as electron donors (ED) in organic photovoltaic cells (OPVC) employing them as anode an buffer layer (ABL) MoO<sub>3</sub>/CuI between the anode and the polymer [12,13]. On the other hand we have studied the agent oxidant/monomer ratio in order to synthesize the optimum redox state in the PANI derivatives which can be applied in heteroarylanilines so as to improve the photovoltaic yield.

The synthesized polymers were Poly(4-Aminoindole) (P4AI<sub>n</sub>) and poly(4-Aminoindane) (P4AI), both synthesized for the first time, and poly(2-ethylaniline) (P2EA) and poly(2-propylaniline), previously synthesized [13-26], were studied Figure 1. To this purpose it is essential to obtain the optimum amenable oxidant/monomer ratio in order to observe this last via UV-Vis spectroscopy and FT-IR.

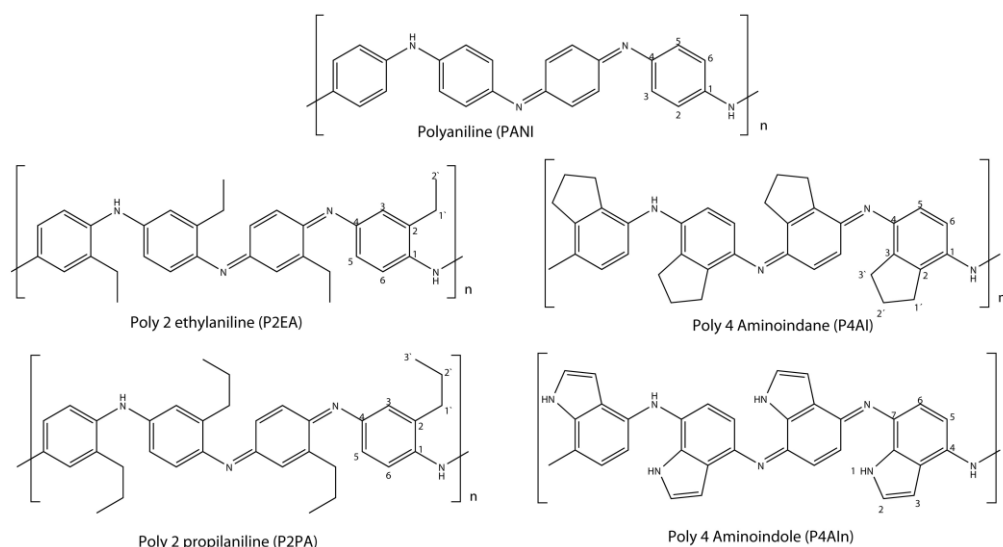


**Figure 1.** Structure of PANI and its derivatives

## EXPERIMENTAL

### Chemical synthesis of PANI and its derivatives

2-ethylaniline (2EA), 2-propylaniline (2PA), 4-aminoindane (4AI), 4-aminoindole (4AIIn) and ammonium persulfate ((NH<sub>4</sub>)<sub>2</sub>S<sub>2</sub>O<sub>8</sub>) were purchased from Aldrich and used as received. Aniline was vacuum distilled twice before using in its polymerization.

PANI derivatives were synthesized following the same procedure [27, 28]. Both aniline and each of its derivatives (2EA, 2PA, 4AI, 4AIIn) were dissolved in 1 M HCl, varying the oxidant/monomer ratio from 1:1 to 4:1 in each synthesis.

Each reaction was carried out under constant stirring for 24 h at 25 ° C. Then each precipitate was filtered and washed with 1 M HCl to remove small amounts of unreacted oligomers and monomer. Finally the precipitate was washed with absolute ethanol (200 mL). Each synthesized polymer was neutralized with 25% NH<sub>4</sub>OH (50 mL) under constant stirring for 24 h in order to obtain it in its ground state (undoped). Once the undoped polymer was filtered, it was washed with 25% NH<sub>4</sub>OH and vacuum dried at 60° C to constant mass.

### UV-vis and FT-IR characterization of PANI and its derivatives

UV-Vis spectra were obtained on an Analytikjena SPECORD 40 spectrophotometer in a 1 cm optical path quartz cell. DMSO was used as solvent for all polymers. Spectra were run respectively for the polymer in undoped state to detect changes in absorbance due to

the existence quinoids units. For optical  $E_g$  measurements an approximation of the Tauc equation [29-33] was used and, this last, deduced from data obtained by UV-vis spectra as follows:

$$A \approx \frac{B (h\nu - E_g)^{1/2}}{h\nu} \quad \text{Eq (1)}$$

Where A (absorbancy) B is a constant of material, h constant of Planck and  $\nu$  frequency.

If  $A=0$ ,  $h\nu=E_g$  it is possible to deduce the  $E_g$  energy plotting  $(Ah\nu)^2$  versus  $h\nu$ .

FT-IR spectra were recorded on a Bruker spectrometer from KBr pellets containing the corresponding polymer.

### Electrochemical studies

Cyclic voltammetry (CV) is a powerful tool to experimentally determine HOMO energy [34-38]. Electropolymerization of each monomer was performed using a Voltmaster, model CV-50W potentiostat. A conventional three-electrode electrochemical cell was used. The working electrode was a  $0.07 \text{ cm}^2$  platinum disc. The counter electrode was a platinum coil. All potentials quoted in this paper are referred to an Ag/AgCl electrode that matches the potential of a saturated calomelane electrode (SCE) at room temperature. Before and during electropolymerization, all monomer solutions were deaerated by purging them with high purity argon. A 0.05 M solution of aniline and its derivatives in 0.5 M  $\text{H}_2\text{SO}_4$ , that also acts as supporting electrolyte, was employed to perform the electrochemical study of the polymers under survey. The electropolymerization was accomplished by CV using  $50 \text{ mV s}^{-1}$  scan rate and 10 successive cycles between  $-0.2$  and  $1.4 \text{ V}$ . For 4AIn polymerization, the potential window used was between  $-0.2 \text{ V}$  and  $1.2 \text{ V}$  because indole polymerizes at potentials above  $1.2 \text{ V}$  [39-41], this ensures that the polymerization takes place only through aniline nitrogen.

### HOMO experimental determination

The main issue of this study is the potentiodynamic profile that provides information about the electrical behavior of the polymers, allowing HOMO and onset oxidation potential to be correlated.

Using quantum chemical calculations a slope change of the anodic current in a CV, called the onset oxidation potential ( $E_{\text{ox}}^{\text{on}}$ ), linearly correlates with HOMO energy

( $E_{HOMO}$ ), at a correction factor of 4.4 eV for a SCE. Thus, the equation to be applied for HOMO calculation by the electrochemical method is as follows [35]:

$$E_{HOMO} = - ((E_{ox})^{on} + 4.4) \text{ eV} \quad \text{Eq (2)}$$

### Deposit of ED on OPVC

OPVCs studied the multi-heterojunction: ITO (Indium Tin oxide)/ABL /ED/C<sub>60</sub> /BCP /Al. In these cells, fullerene (C<sub>60</sub>) and BCP (bathocuproine) have been used as electron acceptor and exciton blocking layer (EBL), respectively. C<sub>60</sub> is well known as a very efficient electron acceptor. Between the C<sub>60</sub> and the aluminum cathode, the introduction of EBL improves significantly the OPV cell's performances [42]. The ABL was either MoO<sub>3</sub>/CuI. [43]

Before thin films deposition, the ITO coated glass substrate was placed in the vacuum chamber (10<sup>-4</sup> Pa). The ABL, ED, C<sub>60</sub>, BCP layers were deposited onto the substrate by sublimation and Al was deposited via high vacuum evaporation, without breaking the vacuum. The CuI layer thickness was 3 nm, as per earlier work [44], while the MoO<sub>3</sub> layer was 4 nm thick [45]. The thickness of the different ED layers has been optimized experimentally. It is, whatever the ED used, 15 nm. Finally, the thickness of the ED, C<sub>60</sub>, and BCP films was 15 nm, 40 nm and 9 nm respectively. The deposition rate of the organic material was 0.05 nm/s. The effective area of each cell was 0.16 cm<sup>2</sup>. The thin films thicknesses and deposition rates were estimated *in situ* using a quartz monitor. Finally, the cell arrangement was:

glass/ITO(100nm)/ABL/ED/C<sub>60</sub>(40nm)/BCP(9nm)/Al(100nm).

In the OPVC (a new purification occurred) Indeed, it has been shown that, using the same charge in the evaporation crucible, there is an "auto purification" of the product [46].

All polymers employed in the photovoltaic devices were undoped. Device preparation was done by sublimation (thermal evaporation) at 1x10<sup>-5</sup> torr. The thin film deposition rates and thickness were estimated *in situ* with a quartz monitor. Electrical characterization was carried out with an automated I-V tester, in the dark and under sun global AM 1.5, simulated solar illumination. Photovoltaic cell performance was measured using a calibrated solar simulator (Oriel 300W) at 100 mW/cm<sup>2</sup> light intensity.

## RESULTS AND DISCUSSION

### UV-Vis spectroscopy

The emeraldine redox form of PANI, is attained when synthesized using a  $(\text{NH}_4)_2\text{S}_2\text{O}_8/\text{aniline}$  ratio between 1:1 and 1.25:1 [47, 48]. In the present case the emeraldine state was obtained with a 1:1 ratio. Figure 2 shows the UV-Vis spectrum of PANI alquilderivatives. Two distinctive absorption maxima corresponding to  $\pi-\pi^*$  benzenoid electronic transitions, at around 300 nm (333 nm), and to  $\pi-\pi^*$  quinoid electronic transitions at about 600 nm (628 nm) are observed. In this wavelength range,  $n-\pi^*$  transitions also exist owing to electrons in nonbonding orbitals of the imino nitrogen formed by the quinoid rings [49].

It is possible to observe that with increasing oxidant/monomer ratio for polymers, the absorbance of quinoids increases up to a point where the over oxidation occurs at oxidant/monomer ratio of 4 Figure 2. This occurs because when the optimum oxidant/monomer ratio is exceeded and PANI derivatives in its over-oxidized state (pernigraline) it possesses one benzenoid unit for every quinoid unit. This excess of quinoids units hinders  $n-\pi^*$  transitions due to Fermi level transitions [50-52].

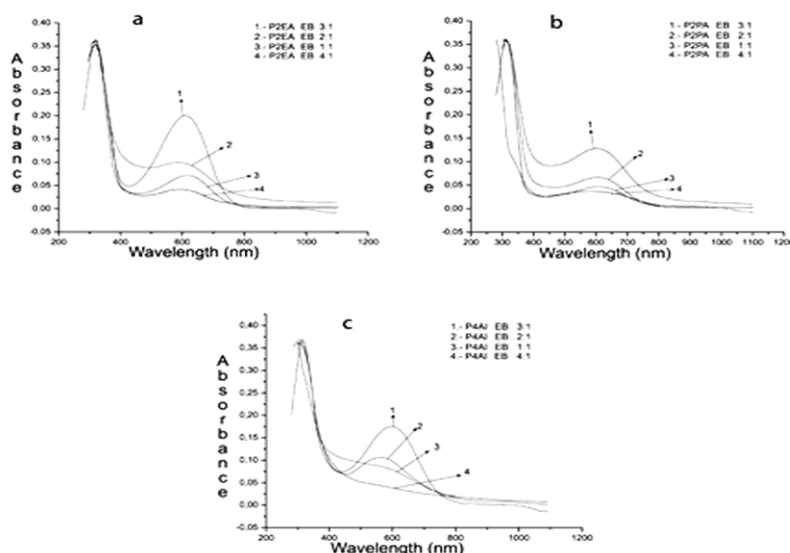


**Figure 2.** UV-Vis spectra of PANI derivatives at different oxidizing agent concentration in DMSO

Quinoid transitions increase as the oxidant/monomer ratio increases; however, when the 4:1 ratio is reached a drastic drop takes place Figure 2. This suggests that molecule oxidation is hindered since a greater concentration of oxidizing agent per monomeric

unit is required to obtain an oxidized state close to that of PANI EB. The optimum benzenoid:quinoid absorbance ratio (1.46) cannot be obtained with any of these three polymers, Figure 3, because these substituents (ethyl, propyl indane and indole groups) hinder quinoid units formation.

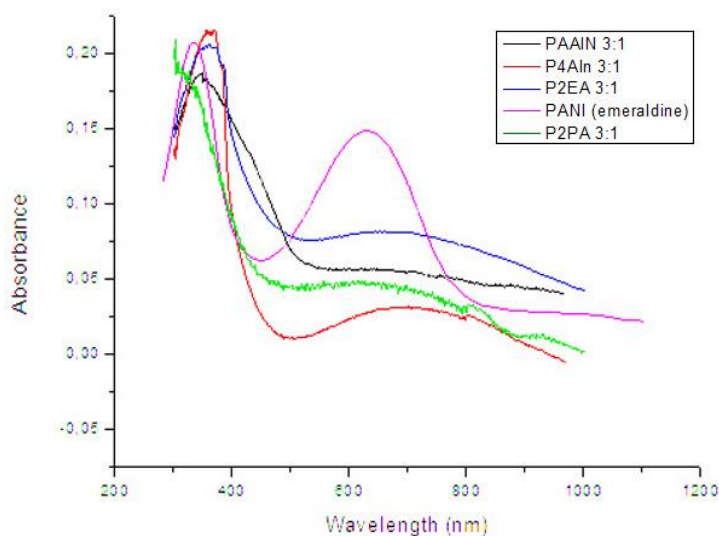


**Figure 3.** UV-vis spectra of PANI derivatives in optimal redox state achieved

### FT-IR spectroscopy

All spectra of the studied polymers, Figure.4, show a band at around  $3200$  and  $3500\text{cm}^{-1}$  corresponding to NH stretching, and two bands near  $1600$  and  $1500\text{ cm}^{-1}$  for  $\text{N}=\text{Q}=\text{N}$  and  $\text{N}-\text{B}-\text{N}$  stretching where Q and B correspond to quinonic and benzenic rings, respectively. These bands are of great importance in characterizing the polymer as they give information concerning its redox status. Therefore, the emeraldine state is reached when the transmittance ratio between both bands is 1 [53]. On the other hand, unlike PANI spectrum, P2EA, P2PA and P4AI exhibit bands between  $2870$  and  $2970\text{ cm}^{-1}$  corresponding to C-H stretching of the alkyl chains, Figure 4

The bands at  $1300$  and  $1230\text{ cm}^{-1}$  correspond to C-N stretching and in plane bending of the quinoid and benzenic hydrogens, which is consistent with the  $1600$  and  $1500\text{ cm}^{-1}$  signals, corroborating the existence of quinoid units within the synthesized polymers.

Bands between  $800$  and  $833\text{ cm}^{-1}$ , corresponding to out of plane bending of quinoid and benzenoid hydrogens, were observed in all spectra.

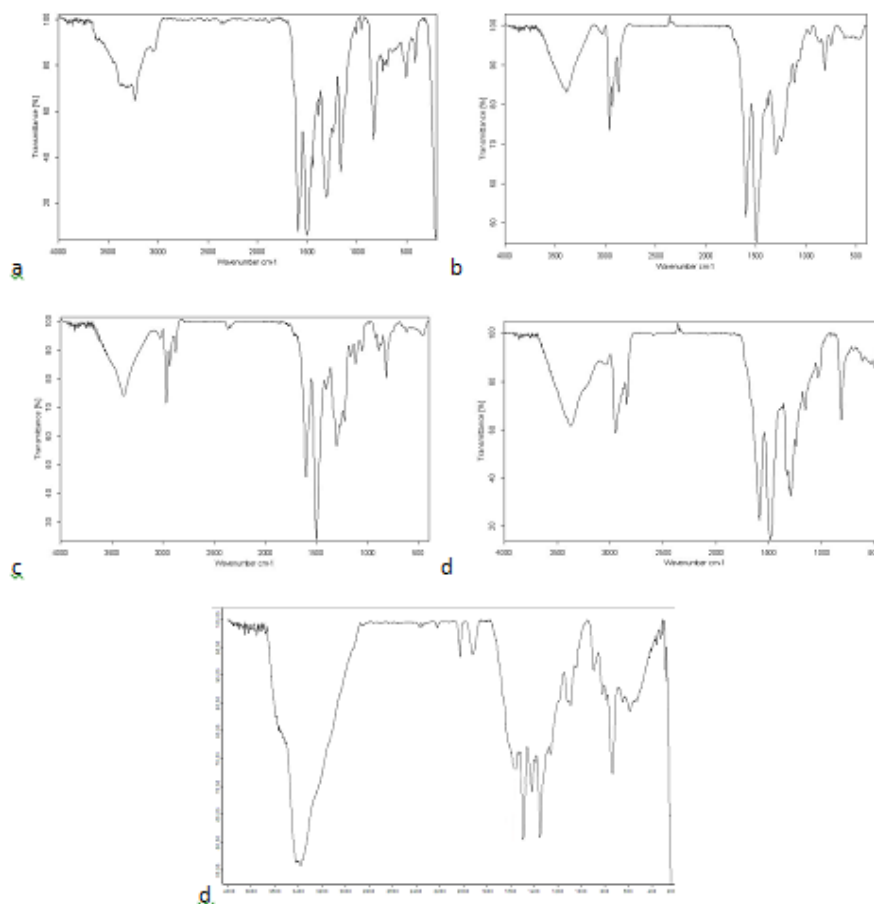


**Figure 4.** FT-IR spectra (a) PANI, (b) P2EA, (c) P2PA, (d) P4AI, (e) P4AIIn

As for P4AIIn, Figure 4e, there is a high intensity band around  $3400\text{ cm}^{-1}$  corresponding to the stretching of both N-H groups (indolic and benzenic). Furthermore, in this region, nearing  $3030\text{ cm}^{-1}$ , C-H stretching of the indole ring appears. Because these three types of vibration occur in this region, a more intense band compared to the rest of polymers is obtained. Moreover, two bands at *ca.*  $2000\text{ cm}^{-1}$  corresponding to overtone of the out-of-plane bending of C-H ( $800\text{ cm}^{-1}$ ) of the aromatic ring were observed [54].

To analyze the polymer redox state, the transmittance of the quinoid band at  $1600\text{ cm}^{-1}$  (Q) and  $1500\text{ cm}^{-1}$  (B) will be compared. Figure 4 shows that for PANI, the B/Q transmittance ratio is 0.98 and 0.95 respectively, indicating that it is in the emeraldine state. These data are consistent with the redox state determined by UV-Vis spectroscopy (1.46)

B/Q relationships for P2EA, P4AI, P2PA and P4AIIn are consistent with those obtained via UV-Vis spectroscopy. This demonstrates that PANI has a greater proportion of quinoid units than the rest of the alkyl derivatives. In addition, P2EA and P4AIIn intensity bands at 600 nm present lower absorbance than PANI.

The fact that P2PA has a lower amount of quinoid units can be explained because, besides having large volume, the propyl group presents a free rotation in the plane, generating higher steric hindrance than P2EA and P4AI, thereby hampering the oxidation of the polymer chain.

Consequently, these data support the results obtained via UV-Vis FT-IR spectroscopy, corroborating that the alkyl substituents hinder polymeric chain oxidation possibly due to steric hindrance.

### Electrochemical Properties

In order to estimate HOMO energy, the slope change of the anodic current was determined as shown in Figure 5. This value corresponds to the onset oxidation potential  $(E_{ox})_{on}$ , and linearly correlates with HOMO energy ( $E_{HOMO}$ ), at a correction factor of 4.4 as eq 2 indicates [29-33]

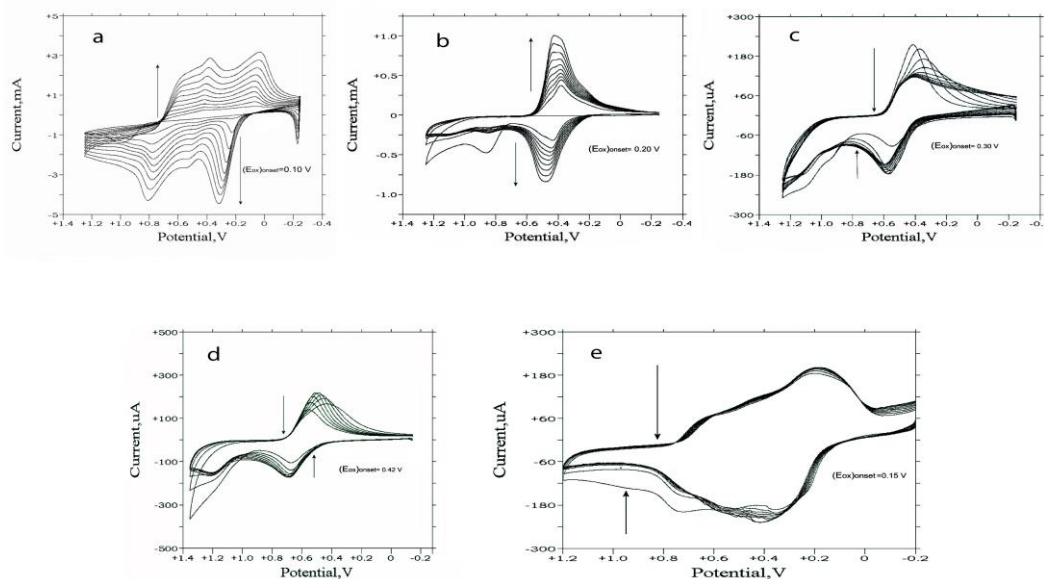


**Figure 5.** Cyclic voltammogram of all PANI derivatives. (a) PANI, (b) P2EA, (c) P2PA, (d) P4AI, and (e) P4AI. (as an analytic equipment was employed, the sweep direction is from right to left and the anodic peak is depicted in the lower part of the CVs)

HOMO values are quoted in Table 1 and were estimated by using eq 2. In the case of solar cells, after photon absorption and excitation creation, the efficiency of the photo induced charge separation is strongly dependent of HOMO and LUMO values. The

LUMO energy of the donor is higher than that of the acceptor, while the HOMO of the acceptor must be significantly greater than that of the donor.

Polymer	HOMO (eV)	LUMO (eV)	Optical Band gap (E <sub>g</sub> ) (eV)
PANI	-4.50	-1.40	3.1
P4AI <sub>n</sub>	-4.55	-1.35	3.2
P2EA	-4.60	-1.30	3.3
P2PA	-4.75	-0.95	3.8
P4AI	-4.82	-1.52	3.3

**Table 1.** Frontiers orbitals and E<sub>g</sub> energy levels of PANI derivatives

When the donor is excited, the electron promoted to the LUMO will lower its energy by moving to the LUMO of the acceptor. The band offset at the organic hetero-interface between the electron-donor and the electron-acceptor tends to separate the positive and negative charge, this is, an electron in the acceptor and a hole in the donor material. The difference between the ED HOMO and EA LUMO is correlated with Voc of OPVC [7], e.g., it is well known that its maximum value of Voc corresponds to the difference between the HOMO of the ED and the LUMO of the acceptor; therefore, following the results indicated in table 2 and Figure 6 the Voc obtained for all polymer are small due to high levels of HOMO energy. The aforementioned leads us to conclude that the Voc is highly dependent on the intrinsic properties of the polymer type used in the individual cell. This is expected since the electron transfer from the excited donor (polymer) to the acceptor molecule (C<sub>60</sub>) is sensitive to the oxidation potential of the donor polymer.

These results agree well with CV and UV-vis results because when the size of substituent and steric hindrance increases the resistance tends to increase. Most organic materials which currently include polyaniline derivatives suffer from the disadvantage of low carrier mobility, that limits the short circuit current of the cells and therefore their efficiency.

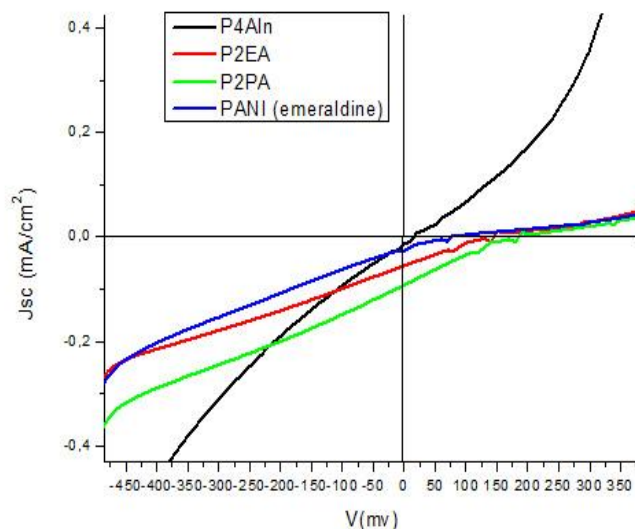


**Figure 6.** J-V graph PANI derivatives (P4AI do not show photovoltaic properties)

The quinoidal units allow the formation of excitation due to the photoexcitation process. PANI in pernigranline redox state and other ramified thiophene aniline polymers have proven to be useless as ED in OPVC due to the absence of quinoid units [10,54] and greater band gaps. In this sense, the optimal redox state or sole presence of quinoids units promote the photovoltaic effect in these polymers, used as ED, Figure 6. For this reason, it is important to know the redox state of the PANI derivatives. In this sense, photovoltaic yield can be increased in our previously synthesized heteroaryl anilines [10] or any other kinds of PANI derivatives. Let it be noted that when PANI derivatives polymers are used as ED, photovoltaic yield of the cells is very low due to their large band gaps and high electrical resistance.

In the case of PANI, it presents the best photovoltaic yield due to optimal redox state Figure 3, 4 and 6. The other polymers show low photovoltaic yields Table 2 due to lower amounts of quinoids units and higher electrical resistance than PANI.

Polymer	Voc (mV)	Jsc (mA/cm <sup>2</sup> )	FF (%)	Photovoltaic Yield
PANI	185	0.094	21	$3.6 \times 10^{-2}$
P4AI	55	0.027	18.4	$2.7 \times 10^{-4}$
P2EA	145	0.057	25.8	$2.1 \times 10^{-3}$
P2PA	190	0.072	22.1	$2.3 \times 10^{-4}$

**Table 2.** Parameters of photovoltaic devices constructed using PANI derivatives as ED

It is important to note that due to the torsion and conformational angle of PANI derivatives these tend to form amorphous thin films in the OPVC, these kinds of packages hinder charge transference and decrease photovoltaic yield [10, 55]. In this sense, there are many factors that affect photovoltaic yield such as the presence of quinoid units (in this kind of polymers), HOMO and LUMO energy, band gap, molecular structure, Voc and the resistance of the polymer.

### Conclusions

PANI derivatives have different abilities to be oxidized and reach an emeraldine-like state, depending on the substitutions they present as well as on the size of the substituent. Thus, as the substituent size increases, the optimum redox state moves away from the emeraldine state and the photovoltaic yield tends to decrease. Consequently, PANI can reach the emeraldine state, because it has no substituents which decrease its potential oxidation. In addition, the high resistance to current flow of this kind of polymers hinders efficient charge transference and decrease photovoltaic yield.

### Acknowledgements

The authors thank FONDECYT financial support through project 1095156 P.Z. acknowledges doctoral scholarship 21090478, doctoral scholarship support 24110046, granted to conduct this research and ECOS CONICYT project No.C09E02 and P. Brassea for his contribution to language support.

### References

- [1] Y.Park, C.Yoon, B. Na, H. Shirakawa, K. Akagi, *Synth. Met.* 41 (1991) 27.
- [2] H. Karami, M.F. Mousavi, M. Shamsipur, *J. Power Sources*, 117 (2003) 255.
- [3] A. Arias, *Polym Rev*, 46 (2006) 103
- [4] E. Sahin, E. Sahmetlioglu, I.M. Akhmedov, C. Tanyeli, L. Toppare, *Org Electron*, 7 (2006) 351.
- [5] S. Varis, M. Ak, C. Tanyeli, I.M. Akhmedov, L. Toppare, *Solid State Sci*, 8 (2006) 1477.
- [6] Y. Ooyama, Y. Harima, *Eur. J. Org. Chem*, 12 (2009) 2903.
- [7] J.C Bernede, *J Chil. Chem Soc*, 53 (2008) 1549.

- [8] R. Kline, M. McGehee, *J. Macromol. Sci*, 46 (2006) 27.
- [9] J.E. de Albuquerque, L. Mattoso, R. Faria, J. Masters, A. MacDiarmid, *Synth Met*, 146 (2004) 1.
- [10] P.P. Zamora, M.B. Camarada, I.A. Jessop, F. R. Díaz, M.A. del Valle., L. Cattin, G. Louarn and J.C Bernede, *Int. J. Electrochem. Sci.*, 7 (2012) 8276.
- [11] J.C. Bernède, L. Cattin, S. Ouro Djobo, M. Morsil, S.R.B. Kanth, S. Patil, P. Leriche, F.R. Diaz, M.A. del Valle, *Physica Status Solidi A*, 208 (2011) 1989.
- [12] P. Kumar, S. Chand, *Progress in Photovoltaics: Research and applications*, 20 (2012) 377.
- [13] V. Shinde, P. P. Patil, *Mat Sci Eng B-Solid*, 168 (2010) 142.
- [14] S. F. Scully, R. Bissessur, D. C. Dahn, G. Xie, *Solid State Ionics*, 181 (2010) 933.
- [15] V. Shinde, A. B. Gaikwad, P. P. Patil, *Surf Coat Tech*, 202 (2008) 2591.
- [16] H. D. Tran, I. Norris, J. M. D`Arcy, H. Tsang, *Macromolecules*, 41 (2008) 7405.
- [17] W. A. Marmisoll, D. Posadas, M. I. Forit, *J. Phys. Chem B*, 112 (2008) 10800.
- [18] B. Gercek, M. Yavuz, H. Yilmaz, B. Sari, *Colloid Surface A*, 299 (2007) 124.
- [19] S. Chaudhari, S. R. Sainkar, P. P. Patil, *Prog. Org Coat*, 58 (2007) 54.
- [20] R. Bissessur, W. White, *Mater. Chem. Phys*, 99 (2006) 214.
- [21] B. Sar, A. Gok, D. Ahn, *J. Appl. Polym. Sci*, 101 (2006) 241.
- [22] A. Falcou, A. Duchene, P. Hourquebie, D. Marsacq, *Synth. Met*, 149 (2005) 115.
- [23] N. A. Zaidi, J. P. Foreman, G. Tzamalis, S. C. Monkman, A. P. Monkman, *Adv. Funct. Mater*, 14 (2004) 479.
- [24] T. Lindfors, A. Ivaska, *J. Electroanal. Chem*, 531 (2002) 43.
- [25] Z. X. Bao, C. X. Liu, P. K. Kahol, N. J. Pinto, *Synth. Met*, 106 (1999) 107.
- [26] Y. Matsuura, Y. Oshima, K. Tanaka, T. Yamabe, *Synth. Met*, 79 (1996) 7.
- [27] F. Cataldo, P. Maltese, *Eur. Polym J*, 38 (2002) 1791.
- [28] D. Yang, P. Adams, B. Mattes, *Synth. Met*, 119 (2001) 301.
- [29] V. Bavastrello, S. Carrara, *Langmuir*, 20 (2004) 969.
- [30] K. Colladeta, M. Nicolasa, *Thin Solid Films*, 451 – 452 (2004) 7

- [31] W. Feng, Z. Qi, Y. Sun, *J. Appl. Pol. Sci*, 104 (2007) 1169.
- [32] B. Sankaran1, J. Reynolds, *Macromolecules*, 30 (1997) 2582.
- [33] S. Bhadra, N. Singha, D. Khastgir, *Eur. Pol. J*, 44 (2008) 1763.
- [34] A. Charas, J. Morgado, J. Martinho, L. Alcácer, S. Lim, R. Friend, F. Cacialli, *Polymer*, 44 (2003) 1843.
- [35] S. Admassie, O. Inganas, W. Mammo, E. Perzon, M. R. Andersson, *Synth. Met*, 156 (2006) 614.
- [36] P. K. Hegde, A.V. Adhikari, M.G. Manjunatha, C.S. Suchand, R. Philip, *Synth. Met*, 159 (2009) 1099.
- [37] Q. Zhang, Y. Li, M. Yang, *J Mater Sci*, 39 (2004) 6089.
- [38] E. Zhou, M. Nakamura, T. Nishizawa, Y. Zhang, *Macromolecules*, 41 (2008) 8302.
- [39] T. Tqken, B. YazVcV, M. Erbil, *Surf Coat Tech*, 200 (2005) 2301.
- [40] M Ghita, D. Arrigan, *Electroanal*, 12 (2004) 979.
- [41] A. Sezai, S. Ozkara, *Int. J Pol Mater*, 53 (2004) 587.
- [42] S.E. Shaheen, C.J. Brabec, *Applied Physic Letters*, 78 (2001) 841.
- [43] L. Cattin, F. Dahou, Y. Lare, M. Morsli, R. Tricot, K. Jondo, A. Khelil, K. Napo, J.C. Bernède, *Journal of Applied Physic Letters*, 105 (2009) 034507.
- [44] C.H. Cheng, J. Wang, G. T. Du, S.H. Shi, *Applied Physics Letters*, 97 (2010) 083305.
- [45] J. Ryu, C. Jang, *J. Org Chem*, 70 (2005), 8956.
- [46] R.F. Slazman, J. Xue, *Organic Electronics*,6 (2005) 242.
- [47] M. Jayakannan, P. Anilkumar, *Eur Polym J*, 42 (2006) 2623.
- [48] E. Iwuoha, S. Mavundla, *Microchimia Acta*, 155 (2006) 453.
- [49] V. Bavastrello, S. Carrara, *Langmuir*, 20 (2004) 969.
- [50] A. Pawlicka, E.C. Pereira, O.R. Nascimento, *Phase Transitions*, 62 (1997) 157.
- [51] D Berner, G. Scheiber, A. Gaymann, H.M. Geserich, P. Monceau, *Journal de Physique IV*, 3 (1993) 255.
- [52] V. M. Souza, L. Walmsley, A. A. Corre, E. C. Pereira, A. L. Gobbi c, *Molecular Crystals and Liquid Crystals*, 374 (2002) 119.

[53] A. Dan, P. K. Sengupta, *J Appl Polym Sci*, 106 (2007) 2675.

[54] L. J. Bellamy, *The infrared spectra of complex molecules*, Willey and Sons 1968.  
pag 68

[54] L. Krinichnyi, *Russian Chemical Bulletin*, 49 (2000) 207.

[55] H. Kim, M. Chandran, S. Park, H. Chae, *Surf. Interface Anal.* (2012) DOI  
10.1002/sia.4988